ACS OMEGA

http://pubs.acs.org/journal/acsodf

Article

Ultrasensitive Electrochemical Immunosensor for Multiplex Sandwich Bioassaying Based on the Functional Antibodies

Li Liu, Xinxin Sheng, Yingying Xue, Zhiyuan Ma, Li Zhang,* Bei Liu,* and Xiaobao Cao*

Cite This: *ACS Omega* 2024, 9, 14249−14254

Read Online

ABSTRACT: In vitro diagnostics (IVDs) based on electrochemical immunosensors are crucial for disease screening, diagnosis, prognosis, and treatment monitoring. However, label-free electrochemical immunosensors commonly suffer from poor specificity, leading to false positives. To address this issue, we propose a highly sensitive and precise electrochemical immunosensor for protein marker detection. This approach involves directly labeling the detection antibodies (Ab_2) with thionine (Thi). The Ab_2 labeled by Thi exhibits a distinct redox peak upon targeted voltage stimulation, enabling accurate quantification of protein biomarkers. Thi-modified antibodies provide significant advantages over traditional antibody modification methods, such as enhanced detection sensitivity, improved accuracy, and specificity in protein marker identification. The method is straightforward and efficient, ensuring specific analyte detection while minimizing interference from other substances in the sample. Additionally, a multielectrode detection method was employed, achieving remarkably low limits of detection (LoDs) for tumor necrosis factor-alpha (TNF-alpha), cardiac troponin I (cTnI), and interleukin-6 (IL-6), with LoDs of 9.38 fg/mL, 1.70 fg/mL, and 8.14 fg/mL, respectively. The proposed electrochemical immunosensor also exhibited high selectivity and repeatability, with relative standard deviations (RSD) of 6.39% for TNF-alpha, 2.42% for cTnI, and 2.72% for IL-6 ($n = 5$). Moreover, it demonstrated high sensitivity and was evaluated for serum detection using the standard addition method. The results highlight the great potential of the proposed electrochemical immunosensor for clinical applications, offering a novel approach for future utilization in clinical settings.

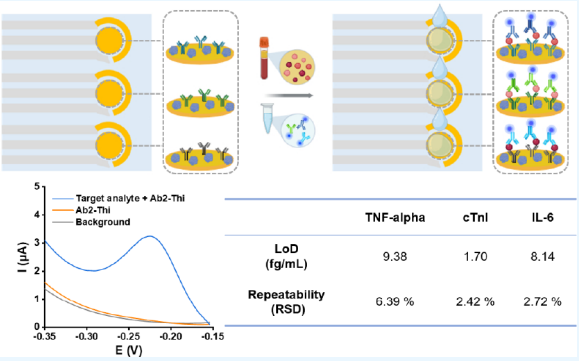

	TNF-alpha	cTnI	IL-6
LoD (fg/mL)	9.38	1.70	8.14
Repeatability (RSD)	6.39 %	2.42 %	2.72 %

■ INTRODUCTION

In vitro diagnostics (IVDs) involve testing blood or tissue samples obtained from the human body.[1,2] These methods are instrumental in advancing personalized medicine, as they allow for the analysis of patients' genotypes, phenotypes, and biomarkers. Such analyses contribute significantly to enhancing treatment efficacy and minimizing adverse reactions.[3,4] Of particular importance is the role of IVDs in early screening and prevention of potentially curable diseases, including various cancers, cardiovascular diseases, and diabetes.[5−8] Additionally, the scope of IVDs extends to encompass clinical medicine,[9] drug research and development,[10] epidemiological investigations,[3,11] and personalized medicine.[3,4]

A wide array of detection methods support IVDs, including enzyme-linked immunosorbent assay (ELISA),[12−14] immunofluorescence analysis (IFA),[4,5] radioimmunoassay (RIA),[15] immuno-PCR,[16,17] photoelectrochemical (PEC),[18,19] nucleic acid hybridization,[20] high-performance liquid chromatography (HPLC),[21] mass spectrometry,[22] electrochemiluminescence,[23−25] fluorescence immunoassay,[26] electrochemical immunoassay[27,28] and so on. Recent research efforts have increasingly focused on the development of advanced IVD devices. The aforementioned methods exhibit advantages, such as high sensitivity, excellent specificity, broad applicability, and rapid result delivery.

Electrochemical immunosensors have become increasingly popular for IVD applications, involving the measurement of electrical signals such as voltammetric, potentiometric, conductometric, and impedimetric signals generated by an electrochemical transductor. These devices are typically designed for user-friendliness and disposability, enabling convenient and rapid on-site measurements. Electrochemical immunosensors, utilizing various detection methodologies, are highly valued in different analytical contexts for their specificity, simplicity, portability, disposability, and capability for in situ or automated detection. Nevertheless, these electrochemical immunosensors encounter certain limitations in their detection processes. For example, label-free electrochemical sensors detect target analytes by monitoring

Received: December 12, 2023
Revised: January 24, 2024
Accepted: February 8, 2024
Published: March 12, 2024

https://doi.org/10.1021/acsomega.3c09942
ACS Omega 2024, 9, 14249−14254

impedance changes.[29−31] However, the presence of impurities on the sensor surface may also cause impedance variations, leading to potential false positive results.

In this study, an electrochemical immunosensor utilizing thionine (Thi) as the electrochemical signal tag for labeling detection antibodies (Ab_2) is reported. This protein double-antibody sandwich assay involves selective capture of the target analyte by capture antibodies (Ab_1), followed by binding with Thi-labeled Ab_2 to form a sandwich structure (Scheme 1). This approach ensures specific detection of the target analyte, minimizing interference from other substances in the sample. The assay was developed for secondary antibody composites to detect tumor necrosis factor-alpha (TNF-alpha), cardiac troponin I (cTnI), and interleukin-6 (IL-6), with limits of detection (LoDs) at 9.38, 1.70, and 8.14 fg/mL, respectively. The determination of these proteins in human serum samples demonstrates significant potential for accurate quantification in clinical analysis.

Scheme 1. Schematic Illustration of the Fabrication Process of Thi-Ab_2 and Electrochemical Immunosensor

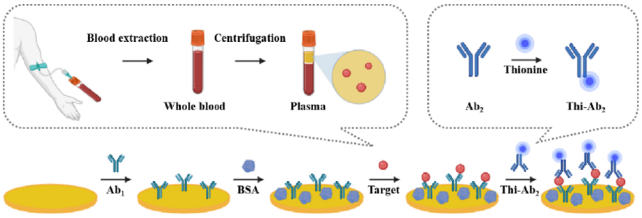

■ EXPERIMENTAL SECTION

Reagents and Chemicals. Thionine (Thi) was obtained from Alfa Aesar Chemical (Shanghai, China). Reagents including *N*-(3-(dimethylamino)propyl)-*N*′-ethylcarbodiimide hydrochloride (EDC), cysteamine hydrochloride (C_2H_7NS-HCl), Tween 20, ethanolamine (C_2H_7NO), potassium ferricyanide ($K_3[Fe(CN)_6]$), potassium ferrocyanide ($K_4[Fe(CN)_6]$), and bovine serum albumin (BSA) were sourced from Aladdin Bio-Chem Technology Co., Ltd. (Shanghai, China). Additional chemicals such as *N*-hydroxysulfosuccinimide sodium salt (NHS), glutaraldehyde ($C_5H_8O_2$), MES buffer, and KCl were produced from McLean Biochemical Technology Co., Ltd. (Shanghai, China). A phosphate-buffered saline (PBS) solution (pH 7.4) was provided by Sangon Biotech (Shanghai) Co., Ltd. (Shanghai, China). Capture antibody (Ab_1) and detection antibody (Ab_2) were prepared by HyTest Biotech Co., Ltd. (Turku, Finland). TNF-alpha antigen was acquired from MedChemExpress Biotechnology Co., Ltd. (New Jersey, United States).

Instrumentation. The mass spectrometer was equipped with an Agilent Jet-stream. All electrochemical experiments were performed on a CHI660E electrochemical workstation in a three-electrode system.

Synthesis of Thi−Ab_2 Composite. Ab_2 (1 mg/mL) was mixed with an EDC/NHS solution and shaken at 650 rpm and 37 °C for 30 min. Subsequently, Thi (1 mg/mL) was added to the mixture, followed by further shake at 650 rpm and 37 °C for 4 h. Next, ultrafiltration using PBS was conducted until the filtrate became clear. The resulting solution was stored at 4 °C for subsequent applications.

Preparation of the Electrochemical Immunosensor. The fabrication process of the immunosensor is shown in Figure S1. The process of cleaning the screen-printed gold electrode (SPGE) was shown in Figure S2. First, we performed cleaning of the SPGE using 0.5 M H_2SO_4. Subsequently, conductivity testing of the electrode was conducted by using $[Fe(CN)_6]^{3-/4-}$. Finally, the cleanliness of the electrode surface was examined using PBS to ensure that it would not interfere with the subsequent tests. The working electrode of SPGE was then modified with cysteamine hydrochloride (C_2H_7NS-HCl, 10 μL, 0.02 M) for 2 h. This was followed by immobilizing glutaraldehyde ($C_5H_8O_2$, 10 μL, 2.5%) on the working electrode surface for 15 min. Subsequently, Ab_1 (10 μL, 1 mg/mL) was applied to the working electrode and allowed to react for 2 h at 4 °C. Ethanolamine (C_2H_7NO, 10 μL, 3.0%) was then added for 15 min at 4 °C. After washing with PBS (pH 7.4) buffer, bovine serum albumin (BSA) solution (10 μL, 1.0 wt %) was applied to the modified electrode at 4 °C for 15 min. The electrode was then rinsed with PBS (pH 7.4) and stored at −20 °C for subsequent detection.

■ RESULT AND DISCUSSION

Feasibility and Optimization of Thi−Ab_2. In Thi solution, a redox peak was discernible, as demonstrated in Figure S3A,B distinctively contrasting with the background. The carboxyl groups (−COOH) on the detection antibody were activated by using an EDC/NHS mixed solution, facilitating a reaction with the amino groups ($-NH_2$) on the Thi molecules. The underlying principle of this reaction is the amide formation of amide bonds between −COOH and $-NH_2$.[32] As depicted in Figure 1A,B, the absence of Thi−Ab_2 resulted in the absence of any discernible redox peak. However, upon modification with Thi−Ab_2, a prominent current peak was distinctly observed. Mass spectrometry analysis was performed to ascertain the molecular weight of the Thi−Ab_2 complex, as demonstrated in Figure S4. The Thi−Ab_2 composites exhibited a peak centered at approximately 152000. The deconvolution molecular weight analysis revealed mass differences between Thi-TNF-alpha and TNF-alpha, Thi-cTnI and cTnI, and Thi-IL-6 and IL-6 to be 4324, 5256, and 4173, respectively. Consequently, the number of Thi molecules linked to different Ab_2 variants was determined to be 16 for TNF-alpha, 19 for cTnI, and 15 for IL-6, confirming the successful synthesis of the Thi−Ab_2 composite. By conducting a UV−vis test, the peaks corresponding to both Ab_2 and Thi on the UV−vis spectra of Thi-Ab_2 indicated the successful conjugation between Thi and Ab_2, as illustrated in Figure S5.

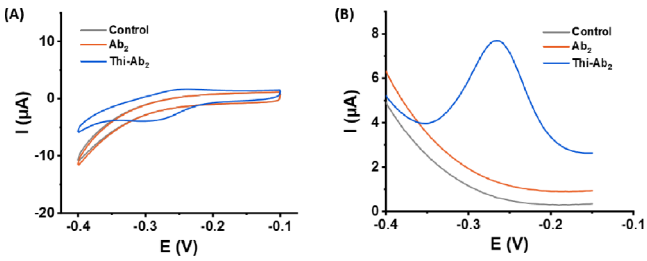

Figure 1. Electrochemical characterization of Thi−Ab_2. (A) CV of Thi−Ab_2. (B) SWV of Thi−Ab_2.

To enhance the electrochemical signal of Thi−Ab_2, we optimized that the composition conditions were optimized. As illustrated in Figure 2A, an increase in the current signal was

https://doi.org/10.1021/acsomega.3c09942
ACS Omega 2024, 9, 14249−14254

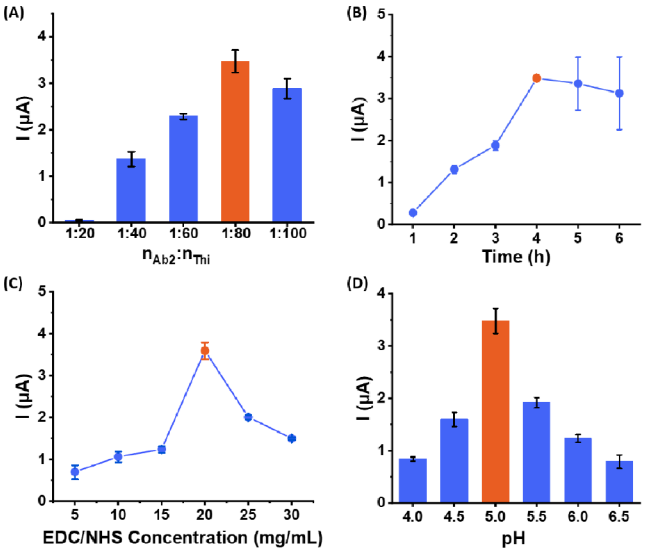

Figure 2. (A) The molar ratio of Ab_2 to Thi. (B) React time optimization for Thi−Ab_2. (C) EDC/NHS concentration optimization. (D) pH value optimization.

observed, with the molar ratio of Ab_2 to Thi ranging from 1:20 to 1:80. Beyond a molar ratio of 1:80, however, the current signal declined with further increases in the molar ratio. This decrease in electrochemical signal at higher molar ratios may be attributed to factors such as excessive modification, steric hindrance, charge shielding effects, or adverse reactions. Therefore, a molar ratio of 1:80 was established as optimal for the synthesis of Thi−Ab_2.

Additionally, it was observed that the peak current was attained at 4 h, after which the signal remained relatively stable with an extended time, as shown in Figure 2B. An insufficient reaction time resulted in an inadequate and uneven reaction between Thi and Ab_2, leading to a reduced electrochemical signal in the Thi−Ab_2 composites. In contrast, excessively prolonged reaction times initiated undesirable side reactions, culminating in nontargeted modifications and reducing the purity of the composites, thus diminishing their electrochemical signal. Figure 2C demonstrated the current trend as a function of the EDC/NHS concentration. For optimal activation, a concentration of 20 mg/mL of EDC/NHS was identified as the most effective. The reduced activation efficiency of EDC/NHS on the −COOH groups of antibodies due to pH variations was primarily attributed to changes in the activity of EDC and NHS, hydrolysis reactions, and alterations in reaction selectivity. Obviously, the synthesis of the Thi−Ab_2 composite was found to be most efficient at pH = 5.0, as shown in Figure 2D.

Principle and Feasibility of Electrochemical Immunosensor. Figure S6A presents the cyclic voltammetry (CV) results in a solution containing 0.1 M KCl and 5 mM $[Fe(CN)_6]^{3-/4-}$ during the electrode modification process. As observed from Figure S6A, the peak current intensity of C_2H_7NS-HCl was notably higher than the background, suggesting successful bonding of C_2H_7NS-HCl onto the SPEC surface via Au−S bonds. Following the modification with $C_5H_8O_2$, Ab_1, and BSA solutions, there was a decrease in the peak current due to coverage of the electroactive sites. This decrease confirms the successful bonding of Ab_1 to the SPEC, indicating the effective fabrication of the electrochemical immunosensor. In Figure S6B, the square wave voltammetry (SWV) curve was utilized to characterize the electrochemical performance of the modified electrode. The alternations in peak current were in agreement with the CV curve, validating the successful immobilization of Ab_1 on the electrode surface and confirming the fabrication of the electrochemical immunosensor.

The detection mechanism for protein markers is illustrated in Figure 3A. Initially, varying concentrations of antigen were

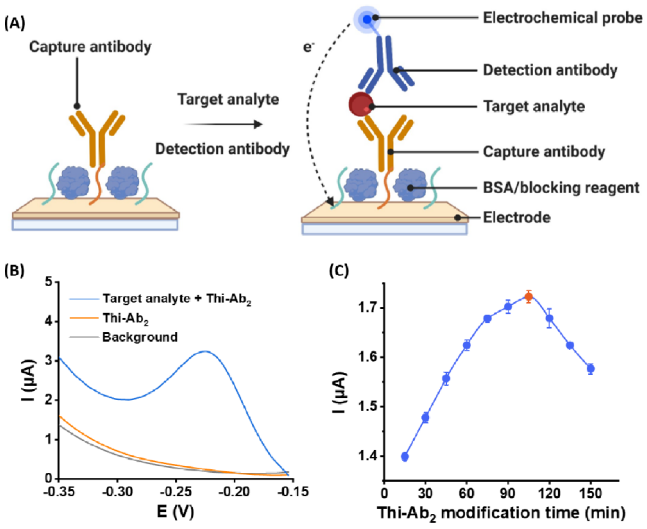

Figure 3. (A) The principle for the detection of TNF-alpha. (B) The feasibility of the detection method. (C) Incubation time optimization for the target and the Thi−Ab_2 mixture.

combined with Thi−Ab_2 composites and incubated in a reactor to form a 'sandwich' structure. Subsequently, the immunosensor was washed with a PBS solution to remove any unbound components. Electrochemical detection was then conducted using an electrochemical workstation in a PBS (pH 7.4) solution. The electroactive groups in the Thi molecule structure facilitated electron transfer within the immunocomplex, yielding discernible electrochemical peaks and amplifying the signal. As shown in Figure 3B, a significant redox peak was observed in the presence of Thi−Ab_2 composites. Additionally, the modification time of the target and Thi−Ab_2 mixture-modified electrode was optimized. The optimal duration, ensuring maximal signal intensity and specificity, was established at 105 min, as demonstrated in Figure 3C. Insufficient modification time on the electrode could lead to weak binding between the labeled molecules and the electrode surface, potentially causing dissociation or inactivation and reducing the electrochemical signal. Conversely, overly prolonged modification times might result in nonspecific adsorption on the electrode surface, producing background signals and uneven label distribution. Therefore, optimizing the modification time was critical to ensure strong binding and minimal nonspecific absorption, crucial for reliable and accurate electrochemical detection.

To detect varying concentrations of TNF-alpha, the electrochemical immunosensor was incubated with TNF-alpha and Thi−Ab_2 in PBS at room temperature for 105 min. Following incubation, the immunosensor was carefully rinsed with PBS to remove any excess target molecules adsorbed on the surface. SWV was employed to detect the electrochemical signals of Thi−Ab_2, and the peak value of the

https://doi.org/10.1021/acsomega.3c09942
ACS Omega 2024, 9, 14249−14254

resultant current signal was recorded for subsequent analysis and quantification. As depicted in Figure 4A, a linear increase

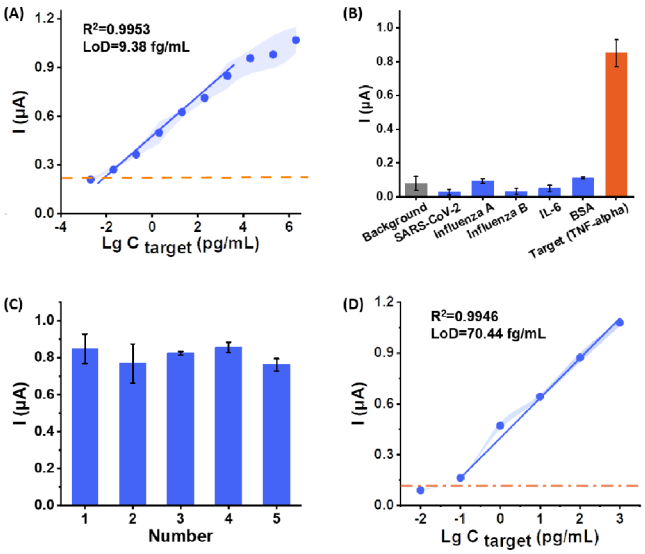

Figure 4. (A) Calibration curve of the immunosensor for the detection of different concentrations of TNF-alpha in PBS. Error bars = RSD (n = 5). (B) Specificity measurement for the immunosensor. 2 ng/mL SARS-CoV-2, 2 ng/mL Influenza A, 2 ng/mL Influenza B, 2 ng/mL IL-6, 2 ng/mL BSA, and 2 ng/mL TNF-alpha. (C) Repeatability of the proposed immunosensor. (D) Calibration curve of the immunosensor for the detection of different concentrations of TNF-alpha in 30% human serum.

in the current peak value was observed corresponding to the logarithmic increase of TNF-alpha concentration over a range from 20 fg/mL to 2 ng/mL. The LoD for the immunosensor was established at 9.38 fg/mL.

Performance and Sample Analysis of the Electrochemical Immunosensor. The specificity of the immunosensor was evaluated using nontarget proteins, including SARS-CoV-2, Influenza A, Influenza B, IL-6, and BSA. The results, represented in the bar graphs of Figure 4B, confirmed the high specificity of the immunosensor.

The repeatability of the electrochemical immunosensor was another essential factor influencing its performance. To assess repeatability, five electrodes were prepared under identical conditions and used to detect 2 ng/mL of TNF-alpha antigen successively, as shown in Figure 4C. The similarity of the SWV signals and a relative standard deviation (RSD) of 6.39% indicated acceptable repeatability of the fabricated immunosensor.

Furthermore, the performance of the immunosensor in clinical applications within complex biological environments was investigated. The feasibility of the immunosensor in serum was assessed by using the standard addition method. Serum was diluted to 30% and then mixed sequentially with various concentrations of TNF-alpha. As depicted in Figure 4D, the LoD for this assay was determined to be 70.44 fg/mL. This LoD demonstrates the capability of the assay to detect ultralow concentrations of TNF-alpha, making it suitable for diverse research and diagnostic applications involving human serum.

Comparative analysis with other reported studies on TNF-alpha immunosensors, as presented in Tables S1 and S4, reveals that the immunosensor developed in this study exhibits a broader detection range and a lower detection limit Additionally, the simplicity of this approach, along with its potential for automation, miniaturization, and portability, offers advantages over other reported methods.

Multielectrode Detection. Figures S7A,B and S8A,B show CV and SWV results in a solution containing 0.1 M KCl and 5 mM $[Fe(CN)_6]^{3-/4-}$ during electrode incubation with anti-IL-6 and anti-cTnI. Figure 5A illustrates the multi-

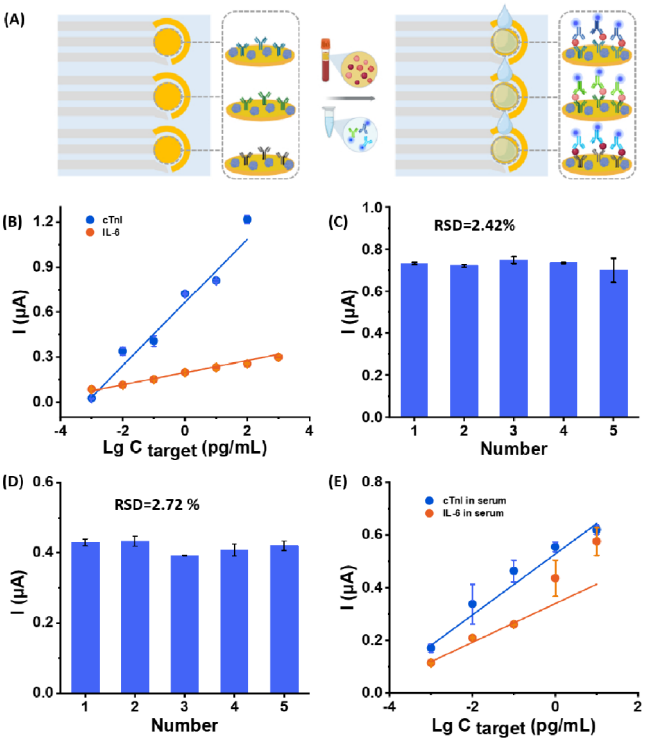

Figure 5. (A) Multielectrode detection. (B) Calibration curve of the immunosensor for the detection of different concentrations of cTnI and IL-6 in PBS. Error bar = RSD (n = 5). (C) Repeatability of the proposed immunosensor (cTnI); (D) repeatability of the proposed immunosensor (IL-6); (E) calibration curve of the immunosensor for the detection of different concentrations of cTnI and IL-6 in 30% human serum.

electrode detection of cTnI and IL-6. This study extended the utility of directly modified Thi−Ab_2 for detecting proteins beyond the initial target, demonstrating the method's versatility and potential. This adaptability for detecting various proteins of interest was further validated. The same methodology was applied to synthesize secondary antibody composites for cTnI and IL-6 detection. The LoDs were established at 1.70 fg/mL for cTnI and 8.14 fg/mL for IL-6, as shown in Figure 5B, indicating the assay's high sensitivity for detecting trace concentrations of these proteins.

To assess the performance of the assay, five electrodes were employed. The repeatability of the measurements demonstrated the RSD of 2.42% for cTnI and 2.72% for IL-6, as illustrated in Figure 5C,D. This consistency and reliability underscore the robustness of the assay system.

The clinical application of the detection system was assessed by measuring standard samples of cTnI and IL-6 in 30% human serum. As illustrated in Figure 5E, the LoDs in serum samples were 17.10 fg/mL for cTnI and 1.38 fg/mL for IL-6, showcasing high sensitivity. These results underline the

https://doi.org/10.1021/acsomega.3c09942
ACS Omega 2024, 9, 14249−14254

method's potential for accurate and sensitive detection of cTnI and IL-6, pertinent to clinical diagnostics and research.

Meanwhile, we performed comparative analysis with previously reported studies on cTnI immunosensors (Tables S2 and S5) and IL-6 immunosensors (Tables S3 and S6), which indicates that the immunosensor developed in this study exhibits broader detection ranges and lower detection limits than those reported in other studies.

■ CONCLUSIONS

An ultrasensitive electrochemical immunosensor based on functional antibodies as signal-producing elements has been designed and prepared. This immunosensor generates electrochemical signals through Thi cross-linked to Ab_2. It offers a highly sensitive detection method for proteins in 30% human serum, which proved to be effective in analyzing various protein markers. By the incorporation of specific antibodies, this sensing platform can be readily adapted for the detection of different target antigens. The electrochemical immunosensor enables sensitive and accurate quantification of TNF-alpha, cTnI, and IL-6, with LoDs of 9.38 fg/mL for TNF-alpha, 1.07 fg/mL for cTnI, and 8.14 fg/mL for IL-6. The electrochemical immunosensor also exhibited high sensitivity, excellent reproducibility, and precision. Looking ahead, these electrochemical immunosensor systems hold significant potential for biomedical applications and real-time biomolecule monitoring.

■ ASSOCIATED CONTENT

Supporting Information

The Supporting Information is available free of charge at https://pubs.acs.org/doi/10.1021/acsomega.3c09942.

Details the fabrication process of the electrochemical immunosensor, its electrochemical characterization, and includes additional figures (Figures S1−S8) and a comparison with other experimental methods (Tables S1−S6), offering comprehensive insights (PDF)

■ AUTHOR INFORMATION

Corresponding Authors

Li Zhang − *Department of Polymeric Materials and Engineering, School of Materials and Energy, Guangzhou Higher Education Mega Center, Guangdong University of Technology, Guangzhou 510006, China*; Email: lizhang@gdut.edu.cn

Bei Liu − *Guangzhou National Laboratory, Guangzhou 510005, China*; Email: liu_bei@gzlab.ac.cn

Xiaobao Cao − *Guangzhou National Laboratory, Guangzhou 510005, China*; orcid.org/0000-0003-2211-2823; Email: xiaobao.cao@hotmail.com

Authors

Li Liu − *Department of Polymeric Materials and Engineering, School of Materials and Energy, Guangzhou Higher Education Mega Center, Guangdong University of Technology, Guangzhou 510006, China; Guangzhou National Laboratory, Guangzhou 510005, China*

Xinxin Sheng − *Department of Polymeric Materials and Engineering, School of Materials and Energy, Guangzhou Higher Education Mega Center, Guangdong University of Technology, Guangzhou 510006, China*; orcid.org/0000-0001-7695-0430

Yingying Xue − *Guangzhou National Laboratory, Guangzhou 510005, China*

Zhiyuan Ma − *Guangzhou National Laboratory, Guangzhou 510005, China*

Complete contact information is available at: https://pubs.acs.org/10.1021/acsomega.3c09942

Author Contributions

L.L. contributed to conceptualization, methodology, writing—original draft, and formal analysis. X.S. contributed to data curation, investigation, and electrochemical immunosensor design. Y.X. contributed to data curation and investigation. Z.M. contributed to investigation. L.Z. contributed to resources, investigation, funding acquisition. B.L. contributed to funding acquisition and writing—review and editing. X.C. contributed to conceptualization, methodology, and writing—review and editing.

Notes

The authors declare no competing financial interest.

■ ACKNOWLEDGMENTS

We gratefully thank the financial support from S&T Special Projects of Guangzhou Laboratory, Grant No. NLPG23-02. In addition, we would like to thank the Proteomics and Metabolomics Platform, Guangzhou Laboratory for our liquid chromatography-time-of-flight mass spectrometry (Q-TOF), and we would be grateful to Nannan Wang for her help in data collection and analysis.

■ REFERENCES

(1) Song, H.; Zhu, Y. The in Vitro Diagnostics Industry in China. *VIEW* **2020**, *1* (1), No. e5.

(2) Turner, A. P.; Chen, B.; Piletsky, S. A. In Vitro Diagnostics in Diabetes: Meeting the Challenge. *Clin. Chem.* **1999**, *45* (9), 1596−1601.

(3) van Pinxteren, L. A. H.; Ravn, P.; Agger, E. M.; Pollock, J.; Andersen, P. Diagnosis of Tuberculosis Based on the Two Specific Antigens ESAT-6 and CFP10. *Clin. Diagn. Lab. Immunol.* **2000**, *7* (2), 155−160.

(4) Banfi, G.; Salvagno, G. L.; Lippi, G. The Role of Ethylenediamine Tetraacetic Acid (EDTA) as in Vitro Anticoagulant for Diagnostic Purposes. *Clinical Chemical Laboratory Medicine* **2007**, *45* (5), 565−576.

(5) Chi, X.; Huang, D.; Zhao, Z.; Zhou, Z.; Yin, Z.; Gao, J. Nanoprobes for in Vitro Diagnostics of Cancer and Infectious Diseases. *Biomaterials* **2012**, *33* (1), 189−206.

(6) Gong, S.; Zhang, S.; Lu, F.; Pan, W.; Li, N.; Tang, B. CRISPR/Cas-Based In Vitro Diagnostic Platforms for Cancer Biomarker Detection. *Anal. Chem.* **2021**, *93* (35), 11899−11909.

(7) Portillo-Lara, R.; Spencer, A. R.; Walker, B. W.; Shirzaei Sani, E.; Annabi, N. Biomimetic Cardiovascular Platforms for in Vitro Disease Modeling and Therapeutic Validation. *Biomaterials* **2019**, *198*, 78−94.

(8) Lian, K.; Feng, H.; Liu, S.; Wang, K.; Liu, Q.; Deng, L.; Wang, G.; Chen, Y.; Liu, G. Insulin Quantification towards Early Diagnosis of Prediabetes/Diabetes. *Biosens. Bioelectron.* **2022**, *203*, 114029.

(9) Guido, M.; Tumolo, M. R.; De Donno, A.; Verri, T.; Serio, F.; Bagordo, F.; Zizza, A. In Vitro Diagnosis of Sepsis: A Review. *Pathol. Lab. Med. Int.* **2016**, *8*, 1−14.

(10) Ebo, D. G.; Leysen, J.; Mayorga, C.; Rozieres, A.; Knol, E. F.; Terreehorst, I. The in Vitro Diagnosis of Drug Allergy: Status and Perspectives. *Allergy* **2011**, *66* (10), 1275−1286.

(11) Lai, C.-C.; Wang, C.-Y.; Ko, W.-C.; Hsueh, P.-R. In Vitro Diagnostics of Coronavirus Disease 2019: Technologies and Application. *J. Microbiol. Immunol. Infect.* **2021**, *54* (2), 164−174.

(12) Qasim, S.; Alamgeer; Saleem, M.; Alotaibi, N. H.; Bukhari, S. N. A.; Alharbi, S. N. A.; Irfan, H. M.; Anwar, R. Appraisal of the Antiarthritic Potential of Prazosin via Inhibition of Proinflammatory Cytokine TNF-α: A Key Player in Rheumatoid Arthritis. *ACS Omega* **2021**, *6* (3), 2379−2388.
(13) Xiong, X.; Liu, L.; Xu, F.; Wu, X.; Yin, Z.; Dong, Y.; Qian, P. Feprazone Ameliorates TNF-α-Induced Loss of Aggrecan via Inhibition of the SOX-4/ADAMTS-5 Signaling Pathway. *ACS Omega* **2021**, *6* (11), 7638−7645.
(14) Herrmann, M.; Veres, T.; Tabrizian, M. Quantification of Low-Picomolar Concentrations of TNF-α in Serum Using the Dual-Network Microfluidic ELISA Platform. *Anal. Chem.* **2008**, *80* (13), 5160−5167.
(15) Poli, C.; Laurichesse, M.; Rostan, O.; Rossille, D.; Jeannin, P.; Drouet, M.; Renier, G.; Chevailler, A.; Tarte, K.; Bendavid, C.; Beauvillain, C.; Amé-Thomas, P. Comparison of Two Enzymatic Immunoassays, High Resolution Mass Spectrometry Method and Radioimmunoassay for the Quantification of Human Plasma Histamine. *J. Pharm. Biomed. Anal.* **2016**, *118*, 307−314.
(16) Zhang, C.; Zhang, P.-Q.; Guo, S.; Chen, G.; Zhao, Z.; Wang, G.-X.; Zhu, B. Application of Biomimetic Cell-Derived Nanoparticles with Mannose Modification as a Novel Vaccine Delivery Platform against Teleost Fish Viral Disease. *ACS Biomater. Sci. Eng.* **2020**, *6* (12), 6770−6777.
(17) Bergallo, M.; Ponti, R.; Gambarino, S.; Galliano, I.; Montanari, P.; Fava, P.; Novelli, M.; Quaglino, P.; Fierro, M. T.; Marra, E. PCR Real time Mismatch Amplification Mutation Assay (MAMA Real Time PCR) for evaluation of TNF-α promoter gene polymorphism -308 G/A in patients with psoriasis. *G. Ital. Dermatol. Venereol.* **2016**, *151* (5), 463−466.
(18) Jia, Y.; Zhang, N.; Du, Y.; Ren, X.; Ma, H.; Wu, D.; Fan, D.; Wei, Q.; Ju, H. Nanoarrays-Propped in Situ Photoelectrochemical System for microRNA Detection. *Biosens. Bioelectron.* **2022**, *210*, 114291.
(19) Jia, Y.; Xu, R.; Xu, K.; Wang, S.; Ren, X.; Zhang, N.; Wu, D.; Ma, H.; Li, Y.; Wei, Q. Ternary Z-Scheme Ag-Embedded TiO2−Ag2S Nanojunction as a Novel Photoelectrochemical Converter for CD44 Detection. *Anal. Chem.* **2022**, *94* (33), 11713−11720.
(20) He, S.; Zhou, Y.; Xie, Y.; Zhang, K.; He, Q.; Yin, G.; Zou, H.; Hu, Q.; Zhang, S.; He, H.; Wang, D. Isothermal Amplification Based on Specific Signal Extraction and Output for Fluorescence and Colorimetric Detection of Nucleic Acids. *Talanta* **2023**, *252*, 123823.
(21) Pan, M.; Lu, Y.; Feng, L.; Zhou, X.; Xiong, J.; Li, H. Absolute Quantification of Total Hemoglobin in Whole Blood by High-Performance Liquid Chromatography Isotope Dilution Inductively Coupled Plasma-Mass Spectrometry. *Anal. Chem.* **2022**, *94* (34), 11753−11759.
(22) Song, D.; Sun, H.; Ma, L.; Liu, J.; Gao, Y.; Zhang, Q.; Xiao, P.; Sun, K.; Shen, M.; Wang, X.; Zhou, M. In-Vitro Diagnostic Reagent Evaluation of Commercially Available Cardiac Troponin I Assay Kits Using H/D Exchange Mass Spectrometry for Antibody-Epitope Mapping. *Anal. Chem.* **2023**, *95* (4), 2278−2284.
(23) Peng, H.; Huang, Z.; Wu, W.; Liu, M.; Huang, K.; Yang, Y.; Deng, H.; Xia, X.; Chen, W. Versatile High-Performance Electrochemiluminescence ELISA Platform Based on a Gold Nanocluster Probe. *ACS Appl. Mater. Interfaces* **2019**, *11* (27), 24812−24819.
(24) Gao, H.; Wang, X.; Li, M.; Qi, H.; Gao, Q.; Zhang, C. Ultrasensitive Electrochemiluminescence Aptasensor for Assessment of Protein Heterogeneity in Small Cell Population. *ACS Appl. Bio. Mater.* **2019**, *2* (7), 3052−3058.
(25) Jia, Y.; Ren, X.; Zhang, X.; Wu, D.; Ma, H.; Li, Y.; Wei, Q. Encapsulation of Tetraphenylethylene Derivative in Liposome Vesicles as Promising Aggregation-Induced Electrochemiluminescence Emitter for Detection of Human Epidermal Growth Factor Receptor 2. *Anal. Chem.* **2023**, *95* (24), 9139−9144.
(26) Mathias, P. C.; Ganesh, N.; Cunningham, B. T. Application of Photonic Crystal Enhanced Fluorescence to a Cytokine Immunoassay. *Anal. Chem.* **2008**, *80* (23), 9013−9020.
(27) Jiang, C.; Alam, M. T.; Silva, S. M.; Taufik, S.; Fan, S.; Gooding, J. J. Unique Sensing Interface That Allows the Development of an Electrochemical Immunosensor for the Detection of Tumor Necrosis Factor α in Whole Blood. *ACS Sens.* **2016**, *1* (12), 1432−1438.
(28) Qi, M.; Zhang, Y.; Cao, C.; Zhang, M.; Liu, S.; Liu, G. Decoration of Reduced Graphene Oxide Nanosheets with Aryldiazonium Salts and Gold Nanoparticles toward a Label-Free Amperometric Immunosensor for Detecting Cytokine Tumor Necrosis Factor-α in Live Cells. *Anal. Chem.* **2016**, *88* (19), 9614−9621.
(29) Wang, Y.; Zhang, Y.; Wu, D.; Ma, H.; Pang, X.; Fan, D.; Wei, Q.; Du, B. Ultrasensitive Label-Free Electrochemical Immunosensor Based on Multifunctionalized Graphene Nanocomposites for the Detection of Alpha Fetoprotein. *Sci. Rep.* **2017**, *7* (1), 42361.
(30) Zhang, R.; Rejeeth, C.; Xu, W.; Zhu, C.; Liu, X.; Wan, J.; Jiang, M.; Qian, K. Label-Free Electrochemical Sensor for CD44 by Ligand-Protein Interaction. *Anal. Chem.* **2019**, *91* (11), 7078−7085.
(31) Aydın, E. B.; Aydın, M.; Sezgintürk, M. K. Impedimetric Detection of Calreticulin by a Disposable Immunosensor Modified with a Single-Walled Carbon Nanotube-Conducting Polymer Nanocomposite. *ACS Biomater. Sci. Eng.* **2022**, *8* (9), 3773−3784.
(32) Maruyama, C.; Toyoda, J.; Kato, Y.; Izumikawa, M.; Takagi, M.; Shin-Ya, K.; Katano, H.; Utagawa, T.; Hamano, Y. A Stand-Alone Adenylation Domain Forms Amide Bonds in Streptothricin Biosynthesis. *Nat. Chem. Biol.* **2012**, *8* (9), 791−797.

https://doi.org/10.1021/acsomega.3c09942
ACS Omega 2024, 9, 14249−14254